

Flame Oscillation Characteristics for Liquid-Centered Swirl Coaxial Injectors^{*}

BAI Xiao, LI Qing-lian, CHENG Peng, CAO Peng-jin

(Science and Technology on Scramjet Laboratory, College of Aerospace Science and Engineering,
National University of Defense Technology, Changsha 410073, China)

Abstract: Gas-liquid swirl coaxial injectors are known to experience self-pulsation easily under certain operating conditions with some special geometrical parameters. Visual combustion experiments in a combustor burning gaseous oxygen (GOX) and liquid ethanol (LET) through a liquid-centered swirl coaxial (LCSC) injector were conducted to explore the effects of self-pulsation on combustion process. High-speed camera captured side-on images of spray and flame simultaneously through the non-contact optical observation method. The effects of both recess length and injection condition on flame dynamics, self-pulsation characteristics and combustion efficiency were analyzed and discussed. With the increase of recess length, flame transforms from stable behavior to self-pulsated behavior with periodic intensity variations in flame emission. Stable flame shows an obvious conical shape, and mainly distributes at the surface of the conical spray, the recirculation zone at the backward facing step of the injection faceplate and the impacting region of spray and combustor wall surface. For the injector with smaller recess length, the self-pulsated flame distributes azimuthally with almost an axisymmetric pattern. Furthermore, flame attaches to the injection faceplate and obviously oscillates radially. However, flame transforms to longitudinal oscillation and detaches from the faceplate when the recess length is large enough. The transition of flame oscillation modes is deemed to be caused by the variation of self-pulsated spray structures. Based on the existed theoretical analysis model, the relationship between flame self-pulsation and flow patterns in recess chamber is analyzed. Self-pulsation of flame and spray is found to be the strongest simultaneously when flow in recess chamber is around the critical mixing flow. Moreover, the efficiency of stable combustion is larger than that of self-pulsated combustion. Recess can improve the combustion efficiency for the LCSC injectors.

Key words: Flame oscillation; Self-pulsation; Recess; Flow pattern; Liquid-centered swirl coaxial injector

CLC number: V434 **Document code:** A **Article number:** 1001-4055 (2021) 07-1593-13

DOI: 10.13675/j.cnki.tjjs.200512

液体中心式气液同轴离心式喷嘴火焰振荡特性

白 晓, 李清廉, 成 鹏, 曹鹏进

(国防科技大学 空天科学学院 高超声速冲压发动机技术重点实验室, 湖南长沙 410073)

摘 要: 气液同轴离心式喷嘴在特定的结构和工况下极易发生自激振荡, 为了探究自激振荡对燃烧过程的影响, 针对液体中心式气液同轴离心式喷嘴, 开展了氧气和酒精的可视化燃烧试验研究。基于非

* 收稿日期: 2020-07-12; 修订日期: 2021-01-07。

基金项目: 国家自然科学基金(11872375); 国家青年科学基金(11802323; 11902351)。

作者简介: 白 晓, 博士, 研究领域为火箭及其组合推进技术。E-mail: zndxbx@163.com

通讯作者: 李清廉, 博士, 教授, 研究领域为火箭及其组合推进技术。E-mail: peakdreamer@163.com

引用格式: 白 晓, 李清廉, 成 鹏, 等. 液体中心式气液同轴离心式喷嘴火焰振荡特性[J]. 推进技术, 2021, 42(7):1593-1605. (BAI Xiao, LI Qing-lian, CHENG Peng, et al. Flame Oscillation Characteristics for Liquid-Centered Swirl Coaxial Injectors[J]. *Journal of Propulsion Technology*, 2021, 42(7):1593-1605.)

接触光学观测方法同步获得了喷雾与火焰的动态结构,研究了缩进长度及喷注工况对火焰的动态特性、自激振荡特性以及燃烧效率的影响。研究发现,随着喷嘴缩进长度的增加,火焰从稳态转变为自激振荡状态。稳态燃烧时,火焰具有明显的锥形分布特征,火焰主要分布于锥形液膜表面、喷嘴出口回流区以及喷雾与燃烧室壁面的撞击区域。对于振荡火焰,当缩进长度较小时,火焰附着于喷注面板上且主要发生径向振荡;而当缩进长度增大到一定程度后,火焰周期性地附着并远离喷注面板且由纵向振荡主导。火焰振荡模式的转变是由自激振荡喷雾结构的变化引起的。基于已建立的理论分析模型,深入分析了火焰自激振荡与缩进室内部流动模态的关系。火焰振荡与喷雾自激振荡强弱同步,且当缩进室内部流动处于临界流动状态时最强。此外,研究发现,稳态燃烧时的燃烧效率大于振荡燃烧状态下的燃烧效率,喷嘴缩进可适当提高燃烧效率。

关键词: 火焰振荡; 自激振荡; 缩进; 流动模态; 液体中心式气液同轴离心式喷嘴

1 Introduction

Combustion instability is manifested by intense pressure fluctuations with large thermal stresses, and is one of the dominating factors that define combustor and engine reliability^[1-3]. Particularly, high-frequency combustion instabilities with kilohertz pressure oscillations can lead to high rates of local heat transfer, vibrations, flashback, variable thrust levels and flame blowout^[4]. The instability in liquid-propellant rocket engines is deemed to be caused by a coupling of the dynamic processes (injection, atomization, vaporization, mixture and chemical reaction) with the response of the gas dynamics in the combustor^[3].

Self-pulsation with high-frequency is an important physical phenomenon occurring in the injector, which is defined as a pressure and flow rate oscillation by a time-delayed feedback between liquid sheet and annular gas^[5]. If pressure oscillation caused by self-pulsation matches with that by combustion instability, the combustion instability in the combustor may be amplified^[6]. So far, self-pulsation has occurred in all types of gas-liquid coaxial injectors during the cold experiments. Bazarov et al.^[5,7] first discovered self-pulsation and put forward the self-pulsation mechanism for the Liquid-centered swirl coaxial injector (LCSC) injector in the 1970s. Then a series of researches began to focus on this phenomenon, including the self-pulsation characteristics^[5,8-10], self-pulsation mechanisms and the effects of self-pulsation on the spray characteristics. It was found that recess length acts as a crucial parameter in self-pulsation^[5]. There is an optimum recess length with which the injector would have the best atomization performanc-

es^[8]. Self-pulsation is the strongest when recess length is around the critical recess length^[9]. The resonance between annular gas and the central air core^[11-12], the dominant wave of the liquid sheet^[13], Kelvin-Helmholtz instabilities^[14-15] and the blocking actions of the conical liquid sheet^[16] are all likely to be excitation mechanisms of self-pulsation. Self-pulsation may sometimes be advantageous for uniformizing the mass flux along radius and increasing the spray angle. However, the SMD increases during self-pulsation, which has negative effects^[17-18].

Except for the researches under cold-test conditions, there is a large number of literature on self-excited oscillations in rocket environments. Flame dynamics during self-excited oscillations have been investigated both by experiments in laboratory-scale combustors^[19-21] and by numerical simulations^[22-24]. Kawashima et al.^[19] observed a ring vortex structure from a single gas-liquid shear coaxial injector of the LOX/methane rocket engine when combustion instability occurs. However, they did not obtain the mechanism probably responsible for these instabilities. Shimizu et al.^[20] found that the flame leading edge was periodically detached from and attached to the injection faceplate during the first-tangential-mode oscillation. Kim et al.^[21] experimentally investigated the beating behavior of acoustically self-excited instabilities in dual swirl combustors. They confirmed that the beating phenomenon occurs due to different fluctuation cycles of the pilot flame and the main flame of a dual swirl combustor. Based on the large-eddy simulation, high-frequency combustion instability in a single-element atmospheric combustor^[22] and an air heater^[23-24] were investigated. The details of flame structures as well as the

unsteady heat release and its coupling with pressure oscillations were captured accurately. It was found that the coupling between the 1T mode oscillation and propellant injection will trigger the pulsating flame behavior in the combustor^[22]. The periodic formation and reaction of ring vortex structures is a basic phenomenon combined with the appearance of self-pulsated flame during combustion^[25]. Therefore, flame dynamics with acoustic excitation were extensively investigated, including GO_2/GH_2 flame^[26], GCH_4/LO_2 flame^[27-30] and premixed turbulent flames^[31-32]. Indeed, these researches are highly beneficial to explore the physical process and mechanisms responsible for combustion instability. Richecoeur et al.^[27-28] experimentally investigated the LOX/GCH_4 flame dynamics based on the external modulations generating high-frequency transverse perturbations. The coupling of acoustics and combustion will notably modify the flow dynamics and enhance the flame expansion rate under specific injection conditions. Kulsheimer et al.^[25] considered that the formation and reaction of large-scale coherent ring-vortex structures are drivers of combustion instabilities for the turbulent premixed swirl flames.

Previous studies on self-pulsation were basically performed under cold-test conditions, a few researches about self-pulsated flame dynamics were aimed at the gas-liquid shear coaxial injectors. Hardly any efforts

were put on self-pulsation characteristics of a LCSC injector under combustion conditions. Whether flame self-pulsation occurs or not during combustion is still unknown. The effects of both recess length and injection conditions on self-pulsated flame dynamics and self-pulsation characteristics have not been clarified. In the present study, the self-pulsated flame characteristics for LCSC injector were investigated experimentally and theoretically. The relationship between flame self-pulsation and flow pattern in the recess chamber was analyzed in depth.

2 Experimental methods

2.1 Experimental facilities

The experimental apparatus is composed of a propellants feed system, a model engine, a LCSC injector, an exhaust system, a pressure and flow measurement system and a Photron Fastcam SA-X2 camera, as shown in Fig.1. Gaseous oxygen (GOX) and pure liquid ethanol (LET) employed as propellants were supplied through a pressurized feed system. High-pressure nitrogen was used to blow away the residual propellants in the liquid ethanol cavity and combustor of the engine for all testing. Using multiple pressure sensors with the accuracy of 0.5% F.S. measure the pressure in liquid and gas manifold as well as combustor. The volume flow rate of LET and GOX were measured by two turbine flowme-

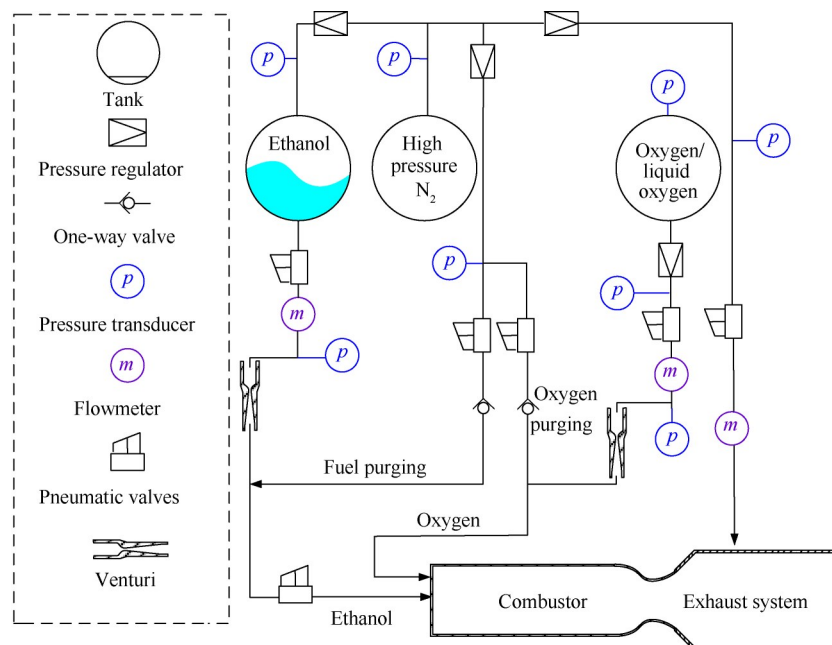


Fig. 1 Experimental facilities and setup

ter with an accuracy of 0.5% F.S., respectively.

Fig.2 shows the test model engine, consisting of the LCSC injector manifold, an optically accessible section for flame visualization, a spark plug, and an exhaust nozzle. The internal combustion chamber is a cuboid with length 160mm, width 32mm and height 50mm. The optical section of the combustion chamber incorporates two 160mm× 50mm quartz glass windows for optical access, one on each side of the combustion chamber, immediately downstream of the injector face.

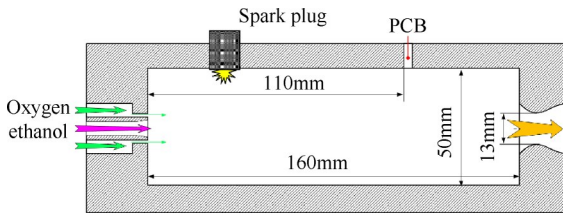


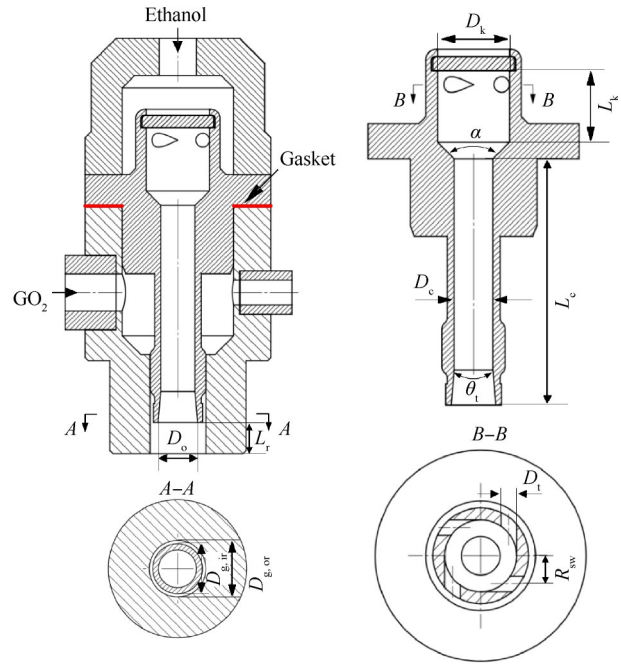
Fig.2 Schematic of the test model engine

The schematic of the LCSC injector is featured in Fig.3, with a detailed view of the liquid pressure swirl injector. The pressure swirl injector adopts four tangential entries to form a swirl motion of liquid. The GOX is injected through an annular aperture between the pressure swirl injector and the outer injector. To investigate the effect of recess length on the flame self-pulsation characteristics of LCSC injectors, three pressure swirl injectors with different discharge orifice length are manufactured. The recess length can be adjusted by increasing the number of gasket with the thickness of 1 mm. The key geometrical parameters are listed in Table 1.

2.2 Experimental techniques

A backlighting photography technique was employed to capture instantaneous spray and flame images, as depicted in Fig.4. The camera exposure time was set to be 12.5μs, and the instantaneous images with 1024×512 pixels were obtained correspondingly. The frame rate was set to be 2×10⁴ frames/s as the best compromise for all experiments.

Considering that the light source changes to red after passing through the red glass, the spray signals only exist in the R channel, while signals emitted by flame distribute in the blue and green band. Researches^[33-34] showed that the averaged B and G values in the RGB model represent well the CH* and C₂* emission of flame.



(a) LCSC injector with manifold (b) Pressure swirl injector

Fig.3 Schematic of LCSC injector

Table 1 Geometrical parameters of a LCSC injector

Parameter	Value
D_c /mm	4.7
L_c /mm	40, 35, 30
$D_{g,ir}$ /mm	8
$D_{g,or}$ /mm	9
D_s /mm	10.2
L_s /mm	10.2
D_r /mm	2.2
R_{sw} /mm	4
α /(°)	90
θ /(°)	10
L /mm	0, 2, 5, 7, 8, 10, 12, 14

To verify this opinion, the background without spray and flame and the histograms of the R, G and B single are shown in Fig.5. The results show that the most pixel gray-values of R channel are greater than 100, while the gray-values of both G and B channels are less than 10. So the effects of surface light on flame image can be neglected. In the present study, flame is modeled by the G and B singles from the high-speed camera.

The self-pulsation frequency can be obtained by processing a series of instantaneous self-pulsated spray and flame images, as shown in Fig.6. First, the raw images with and without spray and flame are used to sub-

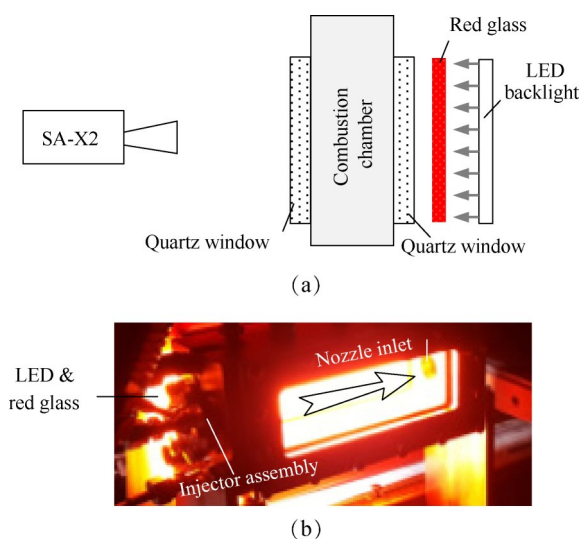


Fig. 4 Optical measurement setup

tract the background. Second, extract the sum gray values of blue channel at four adjacent pixels, where the flame pattern covers periodically. Thus, the sum gray values at certain point in time are obtained. By applying these two steps to a series of instantaneous self-pulsated spray and flame images, the time series of gray values are obtained. Then, the frequency of flame self-pulsation is obtained by the fast Fourier transform of the obtained gray value time series.

2.3 Experimental conditions

The experimental conditions are summarized in Table 2 and Table 3. Experiments in Table 2 were used to analyze the combustion efficiency with the mixture ratio ($r = \dot{m}_{GOX} / \dot{m}_{LET}$) ranging from 0.145 to 0.426. To investigate the effects of recess length on flame stabilization

characteristics, seven typical recess lengths were tested with the high-speed camera in Table 3. For comparative analysis, two repetitive tests were carried out for each experimental condition.

2.4 Experimental setup

The test procedure consecutively triggering the start of the oxidizer flow, fuel flow, ignition and purge for the engine is automated by a timing system. The specific time sequence of the test model engine is depicted in Fig.7. Each test achieves sustained combustion for approximate 0.5s, and the whole process from the beginning of propellant injection to purging after combustion can be recorded by the high-speed camera. Fig.8 shows the representative time histories at main chamber pressures of 0.5MPa, among which, p_{LET} and p_{GOX} represent the pressure of liquid ethanol and gaseous oxygen before injecting, respectively. During the spark discharging, the chamber pressure rises and reaches quasi-steady state ultimately. The system stops supplying fuel at 8.98s. Thereafter ethanol purge opens and chamber pressure decreases gradually. As the valve of gaseous oxygen is closed, chamber pressure decreases rapidly and the engine shuts down.

3 Results and discussions

3.1 Spray and flame patterns

3.1.1 Stable spray and flame patterns

Recess length is a crucial geometrical parameter determining the flow pattern in recess chamber and the

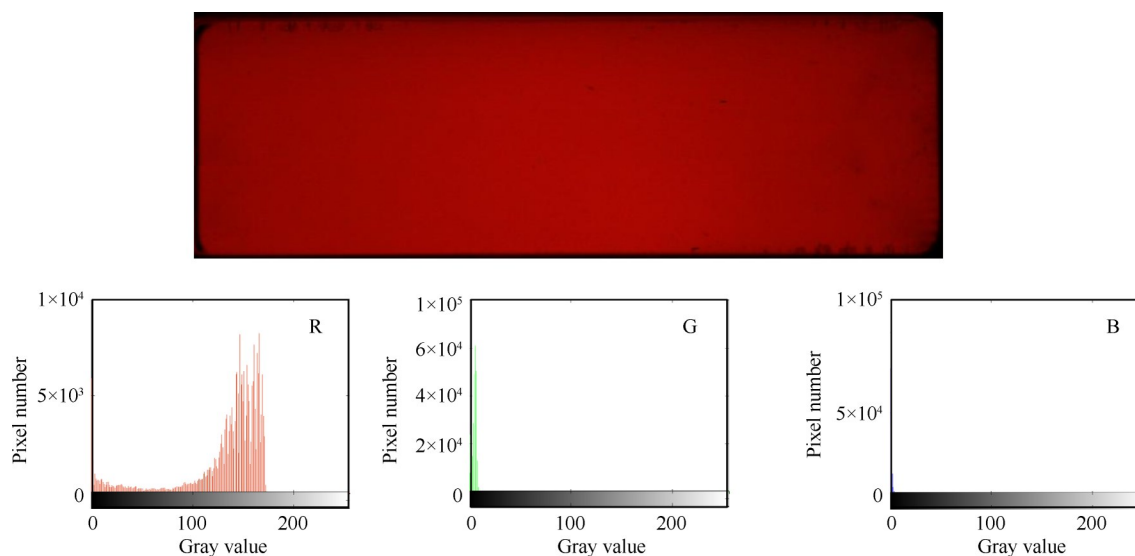


Fig. 5 Background and the histograms of the R, G and B signals

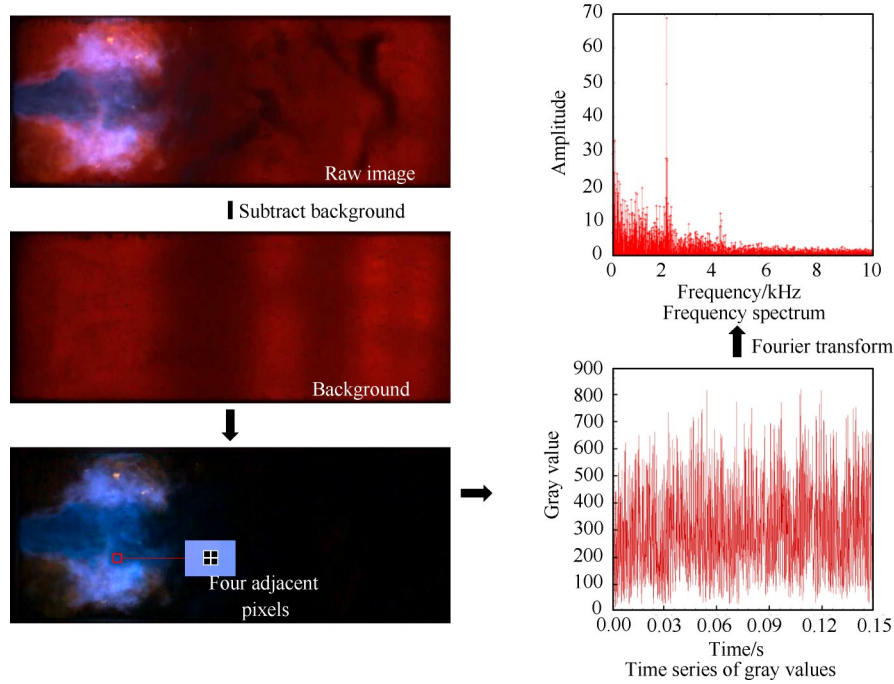


Fig. 6 Frequency extracting method

Table 2 Experimental conditions and parameters for the injector without recess

Test code	$\dot{m}_{\text{LET}}/(\text{g/s})$	$\dot{m}_{\text{GOX}}/(\text{g/s})$	r	p_c/MPa	T_c/K	α	L_r/mm
1	73.7	10.7	0.145	0.449	897	0.070	0
2	70.2	10.5	0.150	0.4361	900	0.072	
3	80.4	16.4	0.204	0.574	963	0.105	
4	72.8	17.2	0.236	0.577	974	0.113	
5	66.8	17.0	0.254	0.574	981	0.122	
6	61.9	15.9	0.257	0.517	979	0.123	
7	57.7	17.2	0.298	0.550	1001	0.143	
8	51.5	16.3	0.317	0.509	1112	0.152	
9	42.5	17.6	0.414	0.516	1044	0.199	
10	49.3	21.0	0.426	0.582	1058	0.204	

Notes: \dot{m}_{LET} and \dot{m}_{GOX} are the mass flow rate of liquid ethanol and gaseous oxygen, respectively. p_c is the chamber pressure. T_c is the chamber temperature. r is the mixture ratio. α is the excess oxygen coefficient.

occurrence of self-pulsation for the gas-liquid coaxial injectors. Based on the backlighting photography technique, instantaneous stable spray and flame images with the recess length L_r of 0 and 2mm are shown in Fig.9. Flame mainly distributes at the boundary of the conical spray, the corner recirculation zone at the backward facing step of the injection faceplate, and the impacting region of spray and combustor wall surface.

The typically stable spray pattern of the LCSC in-

Table 3 Experimental conditions and parameters for the injectors with different recess lengths

Test code	$\dot{m}_{\text{LET}}/(\text{g/s})$	$\dot{m}_{\text{GOX}}/(\text{g/s})$	r	p_c/MPa	T_c/K	α	L_r/mm
11	82.0	16.2	0.198	0.552	950	0.095	2
12	79.8	16.3	0.204	0.532	954	0.098	5
13	81.1	16.3	0.201	0.544	952	0.097	7
14	78.9	16.2	0.205	0.541	955	0.099	8
15	80.5	16.1	0.200	0.548	951	0.096	10
16	82.9	16.6	0.200	0.549	952	0.096	12
17	79.6	15.8	0.198	0.56	949	0.095	14

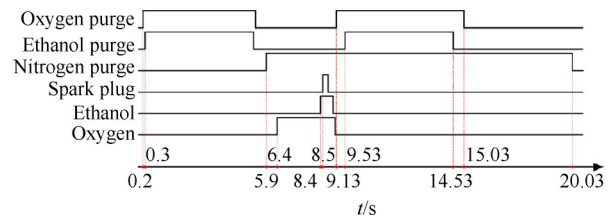


Fig. 7 Time sequence of the test model engine

jector is that a central recirculation region is encompassed by the hollow conical spray. The spray boundary is a significant reference of the investigated flames. The stable flame distribution follows the spray injection pattern and has a conical shape. In the outer region, flame is strongly affected by the annular GOX stream with high injecting velocity, the severe gas-liquid interactions strip numerous liquid droplets from the contiguous spray cone, resulting in the higher local mixture ratio.

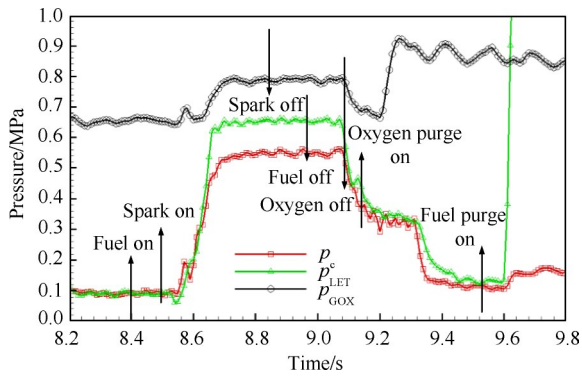


Fig. 8 Time histories of chamber pressure at 0.532MPa and mixture ratio of 0.204

Particularly, large number of ethanol droplets created by the secondary atomization evaporate quasi-instantly, creating rich ethanol/oxygen mixture in the vicinity of the downstream spray. Because the combustor volume is limited, this process mainly locates at the impacting region of spray and combustor wall. Moreover, when spray approaches the side walls of the combustor, the unevaporated droplets with relatively low velocity together with partial droplets stripping from the spray cone are trapped in the corner recirculation zone. Subsequently, these droplets evaporate rapidly benefiting an increased ethanol vapor concentration, which creates proper mixture and then combustion. Besides, when the inner injector is recessed, the presence of the recess region can significantly improve mixing by promoting the interaction of propellants, which contributes to the mixture and evaporation of propellants in combustor. Therefore there are less droplets that are trapped in the corner recirculation zone and then the flame emission is lower.

tion zone and then the flame emission is lower.

3.1.2 Self-pulsated spray and flame patterns

With the increase of recess length, the spray and flame transform from stable behavior to self-pulsated behavior. Fig.10 depicts a sequence of self-pulsated spray and flame images with different recess lengths captured through one full cycle. Except for the difference of flame patterns, whether there is a dominant frequency is the uppermost discriminant standard of self-pulsation. Fig. 11 shows the typical frequency spectrums of self-pulsated and stable flame. Self-pulsation with the order of kilohertz frequency has only been found in the gas-liquid coaxial injectors during the cold experiment before. Now it is confirmed that self-pulsation also occurs in the LC-SC injectors with some special geometrical parameters during combustion.

Previous research^[9] shows that the self-pulsation spray has a Christmas tree shape. However, the self-pulsated spray has no obvious Christmas-tree-like shape during combustion, because the produced droplet clusters experience evaporation and combustion once periodically stripping from the contiguous liquid sheet. The spray oscillations couple with evaporation and chemical reaction in the combustor and finally may amplify combustion instability. Accompanied by the spray oscillation, flame oscillates with periodic intensity variations in flame emission. When recess length is relatively small, the self-pulsated flame appears to distribute azimuthally with a practically axisymmetric pattern as shown in Fig.10(a). In the present study, the distance

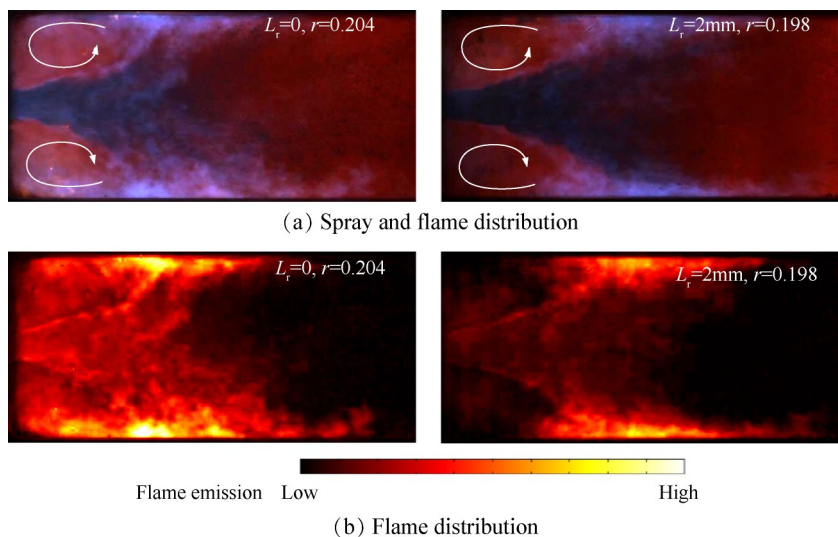


Fig. 9 Instantaneous stable spray and flame images

of the highest flame emission location in the radial direction is used to judge the radial dimension of flame. The specific dimensions have been marked in the figures. It was found that flame attaches to the injection faceplate and obviously oscillates in the radial direction. However, the self-pulsated flame detaches from and attaches to the injection faceplate periodically when the recess length is large enough, as shown in Fig. 10 (b). That means the flame oscillation mode has been transformed and the longitudinal oscillation dominates flame for the injector with large recess. In addition, because recess is beneficial to the mixture and evaporation of propellants in combustor, the existed spray and the distributions of flame emission in combustion chamber decrease with the increase of recess length.

The droplet diameter is usually compared with the thickness of the reaction zone. As a consequence, the atomization qualities (droplet lifetime, diameter and velocity distribution), the spray mass flow rate distribution as well as the interaction of the droplets with the gas turbulence will largely affect the flame behavior^[35]. Cold-tests^[16] showed that spray self-pulsation occurs for the periodic blocking actions of the conical liquid

sheet for the LCSC injectors with certain recess lengths. The recess chamber restricts the expansion of the annular gas stream, then the movement of the conical liquid sheet will also be affected accordingly. When recess length is small, the impeding effects of recess chamber on annular gas and conical liquid sheet are relatively weaker. Thus the liquid sheet and droplets inject with larger radial velocity. With the movement of the droplet clusters, both the horizontal spray width and mass flow rate oscillate periodically. So radial oscillation dominates the flame. However, for the injectors with large recess length, the droplet clusters have almost no radial velocity after the liquid sheet is pushed to the centerline of the injector. The droplet clusters oscillate periodically in the longitudinal direction when injecting from injector. Then flame also oscillates longitudinally.

3.2 Self-pulsation characteristics

The self-pulsation frequency is the frequency at which the spray or flame oscillates. It can be obtained from a series of instantaneous self-pulsated spray and flame images because flame self-pulsation typically accompanies variation in flame luminosity periodically. Based on three thousand instantaneous self-pulsated

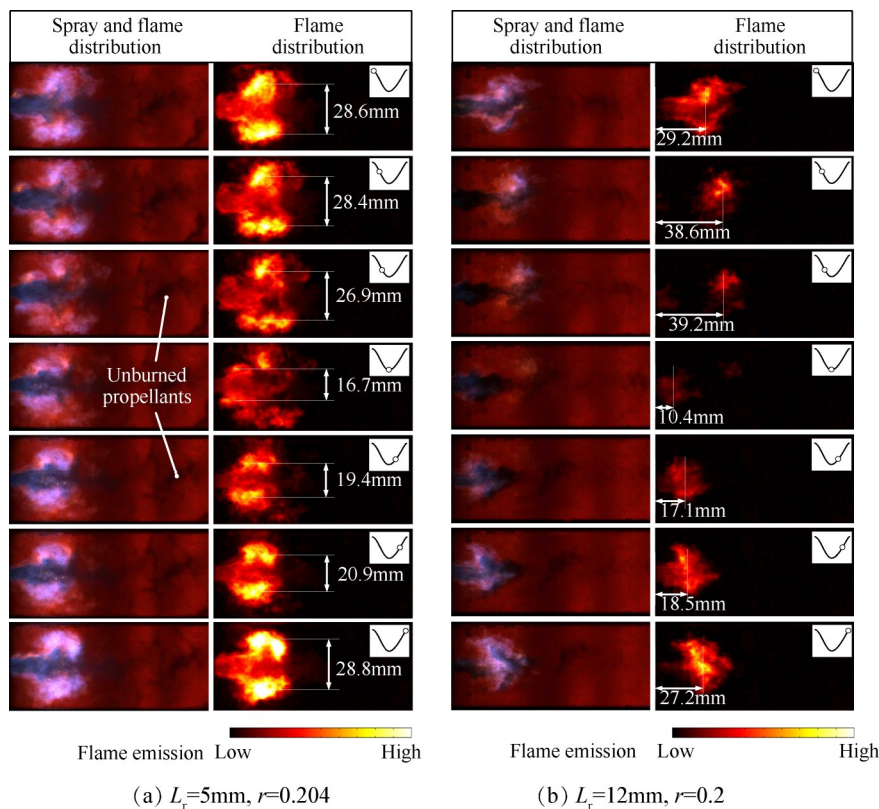


Fig. 10 Self-pulsated spray and flame patterns in one cycle

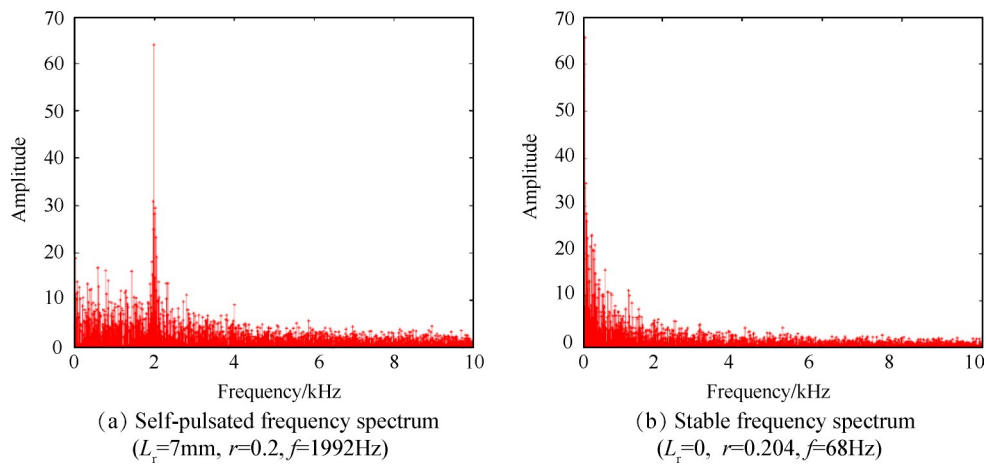


Fig. 11 Typical frequency spectrums for the self-pulsated and stable flame

spray and flame images, the flame self-pulsation frequency and intensity are obtained. Notably, flame pattern and luminosity vary for the injectors with different recess lengths. In order to obtain accurate and exactly comparable data, calculating the self-pulsation intensity at different locations of the whole flame field, the maximum value obtained is chosen as the self-pulsated flame intensity of the current test.

Fig. 12 shows self-pulsation frequency and intensity of flame with respect to recess length with the mixture ratio of 0.2. Recess length has less influence on self-pulsation frequency at about 1980Hz for the injectors with relatively small recess length (5~10mm in the present study). However, when the recess length is large enough, self-pulsation frequency decreases with the increase of recess length. Previous researches^[16] showed that the conical liquid sheet experiences two sub-stages during self-pulsation in one cycle, including the first stage that the liquid sheet approaches the surface of outer injector and the subsequent stage that liquid sheet is pushed to the centerline of injector. These dynamic processes occur in recess chamber and are accompanied by the periodic pressure oscillation of the blocked gas stream. Considering the principal force affecting the movement of liquid sheet, the surface tension forces together with the blocked gas pressure converge the liquid sheet to the centerline of injector. However, the centrifugal forces as well as the interior gas pressure of the central recirculation region diverge the liquid sheet. When the recess length is small, the exterior pressure increases slowly due to the relatively weaker wall constraint of

the recess chamber. However, the effects of wall constraint strengthen gradually when recess length is large enough, the pressure of the blocked gas increases quickly with the liquid sheet approaching the wall of the recess chamber. Therefore, because the resistance increases, the characteristic frequency of the liquid sheet oscillation decreases with increasing the recess length.

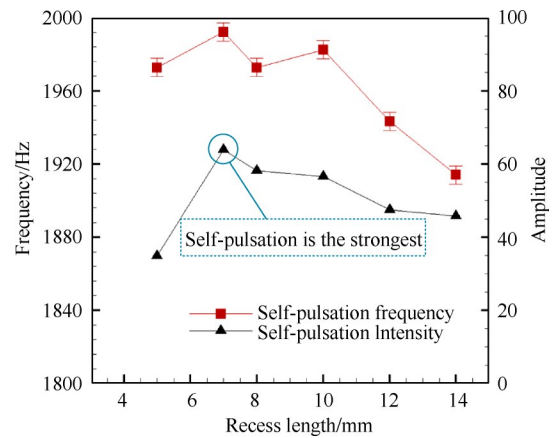


Fig. 12 Self-pulsation frequency and amplitude with recess length ($r=0.2$)

Self-pulsation amplitude increases with the recess length to a maximum and then is followed by a decrease, which means there is a certain recess length under which flame self-pulsation is the strongest. This variety trend is in accordance with the cold-test results^[9]. With the increase of recess length, the flow in LCSC injector experiences the outer mixing flow, the critical mixing flow and the inner mixing flow successively. Self-pulsation is the strongest once flow is close to the critical mixing flow^[9]. In order to further explore the inher-

ent relationship between spray and flame, the flow pattern in recess chamber with different recess length should be confirmed accurately.

3.3 Relationship between self-pulsated spray and flame

Both the geometrical parameters and injection conditions can determine the flow patterns in recess chamber. Based on the researches of Yang et al.^[8] and Kang et al.^[9], the flow pattern in recess chamber can be determined by comparing the liquid film angle and the recess angle. The flow is the critical mixing flow behavior if the liquid film angle (ψ) is close to the recess angle (φ), while it is the outer mixing flow behavior when the recess angle is smaller than the liquid film angle. Otherwise, the flow is the inner mixing flow behavior, as depicted in Fig. 13. The recess angle can be calculated with the following formulation

$$\varphi = 2 \arctan\left(\frac{D_{g,or} - D_o}{2L_r}\right) \quad (1)$$

Based on the momentum conservation equations, the liquid film angle in recess chamber can be inferred, given by

$$\psi = 2 \arctan\left(\frac{\dot{m}_1 u_1 \tan(\psi_1/2) + \dot{m}_g u_g \tan(\psi_g/2)}{\dot{m}_1 u_1 + \dot{m}_g u_g}\right) \quad (2)$$

Where \dot{m}_1 and \dot{m}_g represent the mass flow rate of liquid and gas phase, respectively. The specific solving method of the axial velocity of the gas phase (u_g) and liquid phase (u_1), the spray angle of gas phase (ψ_g) and the spray angle (ψ_1) for the pressure swirl injector with trumpet have been provided in reference[10].

By means of the theoretical analysis model, the liq-

uid film angle in recess chamber can be calculated. The liquid film angle is about 28.04° under the injection condition with the mass flow rate of LET 80g/s and GOX 16g/s, respectively. Fig.14 shows the comparison of the liquid film angle and the recess angle with respect to recess length. The research mentioned above shows that there is a certain geometrical parameter (recess length is 7mm) with which self-pulsation is the strongest with increasing the recess length. The corresponding recess angle is 27.46° , which is basically the same with the liquid film angle at 28.04° . That means flow is the critical mixing flow under this condition. Based on the preceding analysis, the flow for the conditions with smaller recess length belongs to the outer mixing flow, while that for the conditions with larger recess length belongs to the inner mixing flow. Therefore, it can be concluded that self-pulsation of flame follows the spray self-pulsation to the strongest simultaneously, which adds new evidence to the statement that the flame self-pulsation is caused by the spray self-pulsation.

3.4 Combustion efficiency

The combustion efficiency according to mixture ratio for the stable and self-pulsated combustion is shown in Fig.15. The combustion efficiency is calculated by the ratio of the practical characteristic velocity and the theoretical characteristic velocity

$$\eta = \frac{c^*}{c_{th}^*} \quad (3)$$

$$c^* = \frac{p_c A_t}{\dot{m}} \quad (4)$$

Where η represents the combustion efficiency, c^*

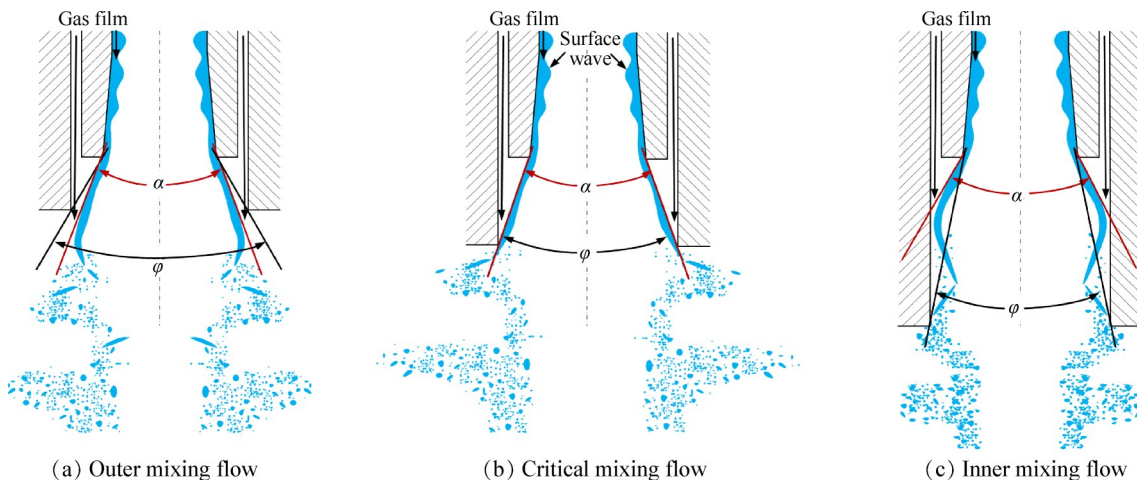


Fig. 13 Flow patterns with different recess lengths

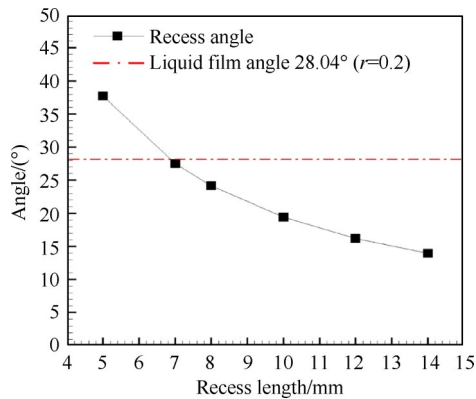


Fig. 14 Comparison of the liquid film angle and the recess angle at various recess length

and c_{th}^* represent the practical characteristic velocity and the theoretical characteristic velocity, respectively. p_c^* represents the total combustor pressure, A_t represents the throat area, \dot{m} represents the total mass flow rate into the combustion chamber.

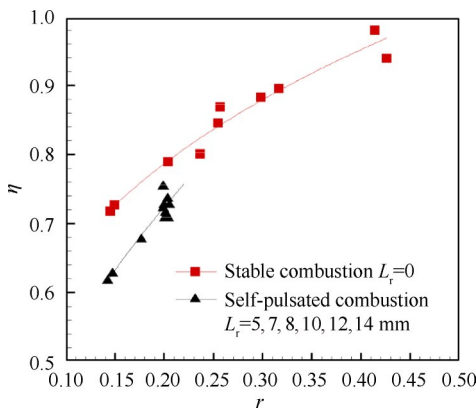


Fig. 15 Comparison of combustion efficiency between stable and self-pulsated behavior

Combustion efficiency increases with the increase of mixture ratio, and is obviously affected by the mixture ratio under fuel-rich conditions. Besides, the efficiency of stable combustion is larger than that of self-pulsated combustion. Self-pulsation occurs coinciding with periodic droplet clusters, meanwhile, horizontal spray width and mass flow rate also vary periodically. The presence of droplet clusters decreases the local mixture ratio. Thus lots of fuel is discharged without burning, resulting in a lower combustion efficiency. Besides, cold-tests^[18] showed that self-pulsation increases the drop size in most of the spray region even when the breakup length is smaller by comparing to the stable spray, which makes negative effect on the vaporization and mixture of propellants thereby reducing combustion

efficiency.

Fig.16 shows combustion efficiency with respect to the recess length, among which all tests are under self-pulsated combustion conditions. Combustion efficiency increases with increasing the recess length. The presence of the recess region can significantly improve mixing by promoting the interaction of propellants, which contributes to the evaporation and mixture of propellants in the combustor. The combustion efficiency increases spontaneously. In addition, the experimental result that the amounts of unburned propellants in combustor decrease with the increase of recess length in Fig.10 also proves this conclusion.

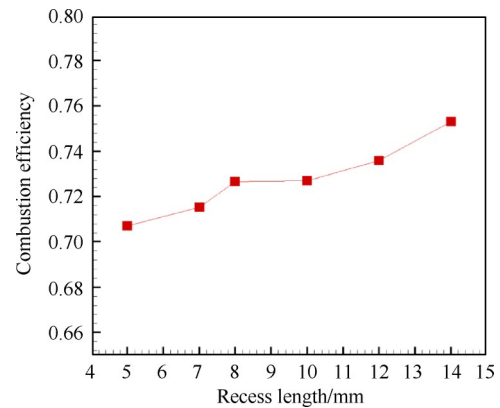


Fig. 16 Combustion efficiency with respect to recess length
($\dot{m}_{LET}=80$ g/s, $\dot{m}_{GOX}=16$ g/s, $r=0.2$)

4 Conclusions

Experimental investigations were conducted to explore the effects of recess length on flame stabilization characteristics generated by a LCSC injector installed in a model combustor.

(1) With the increase of recess length, flame transforms from stable behavior to self-pulsated behavior. Stable flame mainly distributes at the surface of the conical spray, the recirculation zone at the backward facing step of the injection faceplate and the impacting region of spray and combustor wall surface.

(2) Accompanied by the spray self-pulsation, flame oscillates with periodic intensity variations in flame emission. For the injector with small recess length, the self-pulsated flame distributes azimuthally with almost an axisymmetric pattern. Flame attaches to the injection faceplate and obviously oscillates radially.

However, flame transforms to longitudinal oscillation and detaches from the faceplate periodically when the recess length is large enough. The variation of spray self-pulsation structure is deemed to be the cause of different flame oscillation modes.

(3) Recess length has less influence on self-pulsation frequency. When the recess length is large enough, self-pulsation frequency decreases with the increase of recess length. There is a critical recess length with which the flame self-pulsation is the strongest. Based on the existed theoretical analysis model, the relationship between spray self-pulsation and flame self-pulsation is analyzed. Self-pulsation of flame and spray are found to be the strongest simultaneously when flow is around the critical mixing flow.

(4) The efficiency of stable combustion is larger than that of self-pulsated combustion due to smaller drop size. Besides, recess can improve the combustion efficiency for the LCSC injectors.

Acknowledgments: The authors would like to express their sincere thanks for the support from the National Natural Science Foundation of China, the National Science Foundation for Young Scientists of China, the technical support and encouragement of Kang Zhou.

References

- [1] Pomeroy B, Anderson W. Transverse Instability Studies in a Subscale Chamber[J]. *Journal of Propulsion and Power*, 2016, 32(4): 939-947.
- [2] Smith R, Xia G, Anderson W A, et al. Computational Simulations of the Effect of Backstep Height on Nonpremixed Combustion Instability[J]. *AIAA Journal*, 2011, 48(9): 1857-1868.
- [3] Miller K, Sisco J, Nugent N, et al. Combustion Instability with a Single-Element Swirl Injector[J]. *Journal of Propulsion and Power*, 2007, 23(5): 1102-1112.
- [4] Ducruix Sé, Schuller T, Durox D, et al. Combustion Dynamics and Instabilities: Elementary Coupling and Driving Mechanisms[J]. *Journal of Propulsion and Power*, 2003, 19(5): 722-734.
- [5] Bazarov V G, Yang V. Liquid-Propellant Rocket Engine Injector Dynamics[J]. *Journal of Propulsion and Power*, 1998, 14(5): 797-806.
- [6] Im J H, Kim D, Yoon Y, et al. Self-Pulsation Characteristics of a Swirl Coaxial Injector with Various Injection and Geometric Conditions[R]. *AIAA* 2005-3749.
- [7] Bazarov V G. Self-Pulsations in Coaxial Injectors with Central Swirl Liquid stage[R]. *AIAA* 95-2358.
- [8] Yang L J, Ge M H, Zhang M Z, et al. Spray Characteristics of Recessed Gas-Liquid Coaxial Swirl Injector[J]. *Journal of Propulsion and Power*, 2008, 24(6): 1332-1339.
- [9] Kang Z, Li Q, Cheng P, et al. Effects of Recess on the Self-Pulsation Characteristics of Liquid-Centered Swirl Coaxial Injectors[J]. *Journal of Propulsion and Power*, 2016, 32(5): 1124-1132.
- [10] Bai X, Cheng P, Sheng L Y, et al. Effects of Backpressure on Self-Pulsation Characteristics of Liquid-Centered Swirl Coaxial Injector[J]. *International Journal of Multiphase Flow*, 2019, 116: 239-249.
- [11] Huang Y H, Zhou J, Hu X P, et al. Acoustic Model for the Self-Oscillation of Coaxial Swirl Injector[R]. *AIAA* 97-3328.
- [12] Huang Y H, Zhou J, Hu X P, et al. Experiment and Acoustic Model for the Self-Oscillation of Coaxial Swirl Injector and Its Influence to Combustion of Liquid Rocket Engine[J]. *Acta Acustica*, 1998, 23(5): 459-465.
- [13] Im J H, Kim D, Han P, et al. Self-Pulsation Characteristics of a Gas-Liquid Swirl Coaxial Injector[J]. *Atomization and Sprays*, 2009, 19(1): 57-74.
- [14] Eberhart C J, Lineberry D M, Jr R A F. Detailing the Stability Boundary of Self-Pulsations for a Swirl-Coaxial Injector Element[R]. *AIAA* 2013-4064.
- [15] Eberhart C J, Frederick R A. Details on the Mechanism of High-Frequency Swirl Coaxial Self-Pulsation[J]. *Journal of Propulsion and Power*, 2017, 33(6): 1418-1427.
- [16] Bai X, Li Q L, Cheng P, et al. Investigation of Self-Pulsation Characteristics for a Liquid-Centered Swirl Coaxial Injector with Recess[J]. *Acta Astronautica*, 2018, 151: 511-521.
- [17] Im J H, Cho S, Yoon Y, et al. Comparative Study of Spray Characteristics of Gas-Centered and Liquid-Centered Swirl Coaxial Injectors[J]. *Journal of Propulsion and Power*, 2010, 26(6): 1196-1204.
- [18] Kang Z T, Li Q L, Cheng P, et al. Effects of Self-Pulsation on the Spray Characteristics of Gas-Liquid Swirl Coaxial Injector[J]. *Acta Astronautica*, 2016, 127: 249-259.
- [19] Kawashima H, Kobayashi K, Tomita T, et al. A Combustion Instability Phenomenon on a LOX/Methane Subscale Combustor[R]. *AIAA* 2010-7082.
- [20] Shimizu T, Tachibana S, Yoshida S, et al. Intense Tangential Pressure Oscillations Inside a Cylindrical Chamber[J]. *AIAA Journal*, 2011, 49(10): 2272-2281.

- [21] Kim J, Jang M, Lee K, et al. Experimental Study of the Beating Behavior of Thermoacoustic Self-Excited Instabilities in Dual Swirl Combustors[J]. *Experimental Thermal and Fluid Science*, 2019, 105: 1–10
- [22] Matsuyama S, Hori D, Shimizu T, et al. Large-Eddy Simulation of High-Frequency Combustion Instability in a Single-Element Atmospheric Combustor[J]. *Journal of Propulsion and Power*, 2016, 32(3): 628–645.
- [23] Yuan L, Shen C B. Large Eddy Simulation of Combustion Instability in a Tripropellant Air Heater[J]. *Acta Astronautica*, 2016, 129: 59–73.
- [24] Yuan L, Shen C B. Computational Investigation on Combustion Instabilities in a Rocket Combustor[J]. *Acta Astronautica*, 2016, 127: 634–643.
- [25] Klsheimer C, Bchner H. Combustion Dynamics of Turbulent Swirling Flames [J]. *Combustion and Flame*, 2002, 131 (1): 70–84.
- [26] Ghosh A, Diao Q, Young G, et al. Effect of Density Ratio on Shear-Coaxial Injector Flame-Acoustic Interaction [R]. *AIAA 2006-4528*.
- [27] Richecoeur F. Experimentations and Simulations Numeric on Interaction Modes Acoustic Transve at Flames Cryotechniques[D]. *Paris: Ecole Centrale Paris*, 2006.
- [28] Richecoeur F, Ducruix S, Scouflaire P, et al. Experimental Investigation of High-Frequency Combustion Instabilities in Liquid Rocket Engine[J]. *Acta Astronautica*, 2008, 62(1): 18–27.
- [29] Hakim L, Ruiz A, Schmitt T, et al. Large Eddy Simulations of Multiple Transcritical Coaxial Flames Submitted to a High-Frequency Transverse Acoustic Modulation [J]. *Proceedings of the Combustion Institute*, 2015, 35 (2): 1461–1468.
- [30] Hakim L, Schmitt T, Ducruix S, et al. Dynamics of a Transcritical Coaxial Flame under a High-Frequency Transverse Acoustic Forcing: Influence of the Modulation Frequency on the Flame Response [J]. *Combustion and Flame*, 2015, 162(10): 3482–3502.
- [31] Chaudhuri S, Cetegen B M. Response Dynamics of Bluff-Body Stabilized Conical Premixed Turbulent Flames with Spatial Mixture[J]. *Combustion and Flame*, 2009, 156: 706–720.
- [32] Kim KT, Lee J G, Quay B D, et al. Spatially Distributed Flame Transfer Functions for Predicting Combustion Dynamics in Lean Premixed Gas Turbine Combustors [J]. *Combustion and Flame*, 2010, 157: 1718–1730.
- [33] Ballester J, Garcia-Armingol T. Diagnostic Techniques for the Monitoring and Control of Practical Flames [J]. *Progress in Energy and Combustion Science*, 2010, 36 (4): 375–411.
- [34] Huang H W, Zhang Y. Flame Colour Characterization in the Visible and Infrared Spectrum Using a Digital Camera and Image Processing [J]. *Measurement Science and Technology*, 2008, 19(8): 085406.
- [35] Hade R, Lenze B. Measurements of Droplets Characteristics in a Swirl-Stabilized Spray Flam [J]. *Experimental Thermal and Fluid Science*, 2005, 30: 117–130.

(编辑:刘萝威)